processes MDPI

Article

Experimental Test and Feasibility Analysis of Hydraulic Cylinder Position Control Based on Pressure Detection

Rulin Zhou [1], Lingyu Meng [1,2,*] and Xiaoming Yuan [3]

[1] Beijing Tianma Intelligent Control Technology Co., Ltd., Beijing 101399, China; zhourl@tdmarco.com
[2] School of Mechanical Electronic & Information Engineering, China University of Mining & Technology (Beijing), Beijing 100083, China
[3] Hebei Provincial Key Laboratory of Heavy Machinery Fluid Power Transmission and Control, Yanshan University, Qinhuangdao 066004, China; xiaomingbingbing@163.com
* Correspondence: mly929996@outlook.com

Abstract: This paper studies hydraulic cylinder position adjustment controlled by an on–off valve. The aim of this paper is to develop a method of position control for a hydraulic cylinder based on input and output pressure under the mutual coupling feedback of the load and flow, especially in multi-actuator coupling control scenarios. This method can solve the problem of position evaluation and hydraulic cylinder tracking in relation to position detection without a displacement sensor and provide the possibility of automatic adjustment of hydraulic support in the process of intelligent mining. First of all, according to the flow continuity equation and Navier–Stokes equation, a flow model with inlet and outlet pressure is derived. Secondly, the effectiveness of the flow resistance characteristic curve of differential valve is verified by experimental and theoretical analysis. Finally, through experimental verification, when the system pressure is larger than 10 MPa, the error between the actual experimental data and the data calculated by the fitting algorithm is within 5%, which is consistent with the derived formula and proves the validity of the simulation model.

Keywords: position control; hydraulic cylinder; pressure detection; on-off valve; valve spool

Citation: Zhou, R.; Meng, L.; Yuan, X. Experimental Test and Feasibility Analysis of Hydraulic Cylinder Position Control Based on Pressure Detection. *Processes* **2022**, *10*, 1167. https://doi.org/10.3390/pr10061167

Academic Editor: Krzysztof Rogowski

Received: 25 May 2022
Accepted: 6 June 2022
Published: 10 June 2022

1. Introduction

Intelligent mining is a new stage in the development of fully mechanized coal mining technology and also an inevitable requirement of the technological revolution and development of the coal industry [1–4]. In recent years, China's intelligent construction of coal mines has shown positive progress, and the intelligent transformation of the working face has been promoted rapidly. There were only three intelligent working faces in China's coal mines in 2015; the number reached 275 in 2019 and 494 in 2020, with an increase of 80% each year. Nineteen kinds of robot, such as coal mining, anchor drilling and patrol inspection robots, have been implemented and applied in coal mines [5], as shown in Figure 1.

Based on inertial navigation technology, an automatic alignment system of a fully mechanized mining face was developed. The detection error of the straightness of the system was less than 100 mm, and the whole working face alignment error was less than 300 mm [6,7]. The position control of the underground hydraulic support was mainly based on position detection and controlled by a large-flow on–off valve. Although a control valve with switchable large and small flow was developed, it still could not achieve rapidity and accuracy of control [8,9]. Aside from this, the logic cartridge could not effectively remove the need for manual intervention and compensation of hydraulic support in the production process. The main reason was that the displacement sensor could not be installed due to the limitations of the field's applicable conditions, and the position control of the hydraulic cylinder based on the time control of an on–off valve could not be accurately realized, which, thus, became a bottleneck restricting the development of coal mining automation.

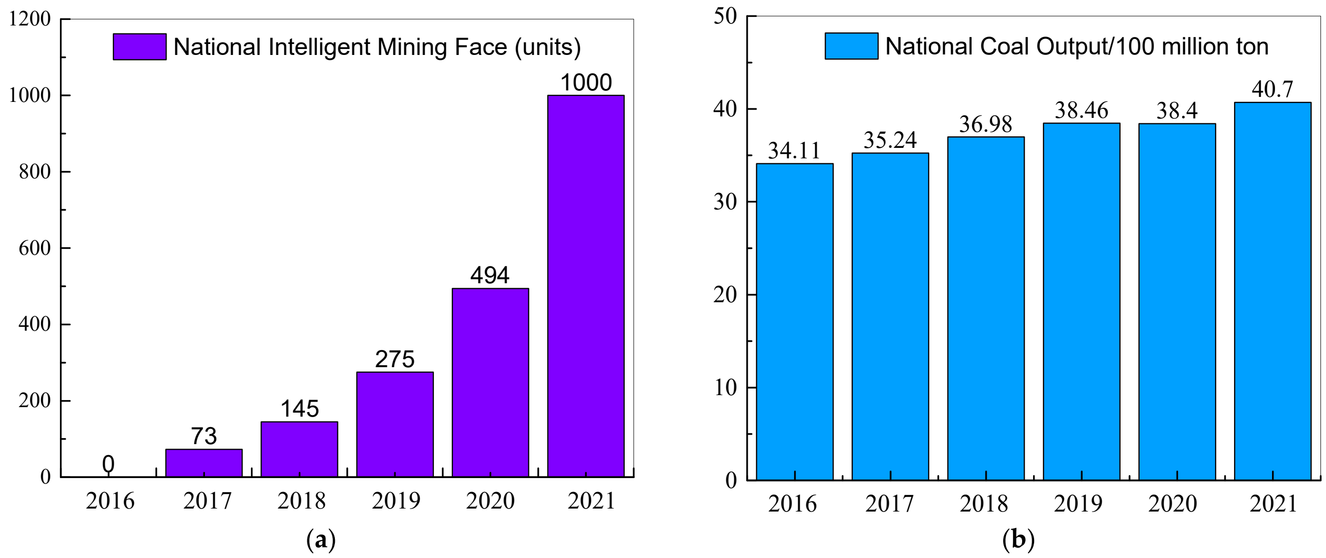

Figure 1. (**a**) Development plan of intelligent working faces; (**b**) Market scale of China's coal industry.

At present, position control systems in the engineering field are mainly electro-hydraulic position servo systems and have been widely used in aerospace [10,11], pump stations [12], water conservancy [13], hydraulic manipulators [14,15] and other fields. Some researchers have also studied high-speed on/off valves in the field of hydraulic engineering [16,17]. However, little research on the position control of hydraulic cylinders based on pressure detection has been conducted [18,19]. In recent years, in order to reduce the cost of valves used in position control systems and improve the scope of application, many scholars have carried out new explorations. Digital hydraulics were integrated into the cylinder, valve, feedback and control to form a fully digital motion characteristic. Digital hydraulic pressure is controlled by electric signal, and digital power amplification is based on hydraulic pressure [20], as shown in Figure 2. Santhosh Krishnan Venkata developed a technique to detect faults in the valve which can lead to better stability of the control loop [21]. Ruan Jian proposed a digital on–off valve based on a stepping motor to convert the rotary motion of the valve spool into axial motion [22], as shown in Figure 3. Zhou Chuanghui put forward an idea to realize the output position control of a hydraulic cylinder through a two-stage, parallel electro-hydraulic position control system based on an electromagnetic directional valve [23]. Jin Liyang studied the control method of hydraulic cylinders with electromagnetic directional valves as the main control element mainly from the perspective of control component modeling, control structure analysis and control algorithms [24]. Pan Min proposed a four-port, high-speed switching valve configuration and investigated the system dynamics and performance [25]. Khayyam Masood implemented a control algorithm to control the speed of a motor with the application of a single sensor [26]. However, the above core technical mechanism was mainly controlled by a feedback control solenoid valve formed by displacement detection, and the system pressure and load were not analyzed, as shown in Figure 4. When the displacement sensor failed, it could not function properly.

In this paper, we built a flow model with inlet and outlet pressure to estimate the position of the hydraulic cylinder. Then, the effectiveness of the flow resistance characteristic curve of differential valve was verified by experimental and theoretical analysis. Finally, the flow model was verified by a valve-controlled cylinder system. The displacement fitting control method based on pressure detection can work normally even when there is no displacement sensor or the displacement sensor fails. It can calculate and estimate the displacement change in real time under the conditions of the existing hydraulic system architecture according to the load change. It is especially suitable for the scenarios where multiple hydraulic cylinders act together under variable load conditions and it is inconvenient to install displacement sensors.

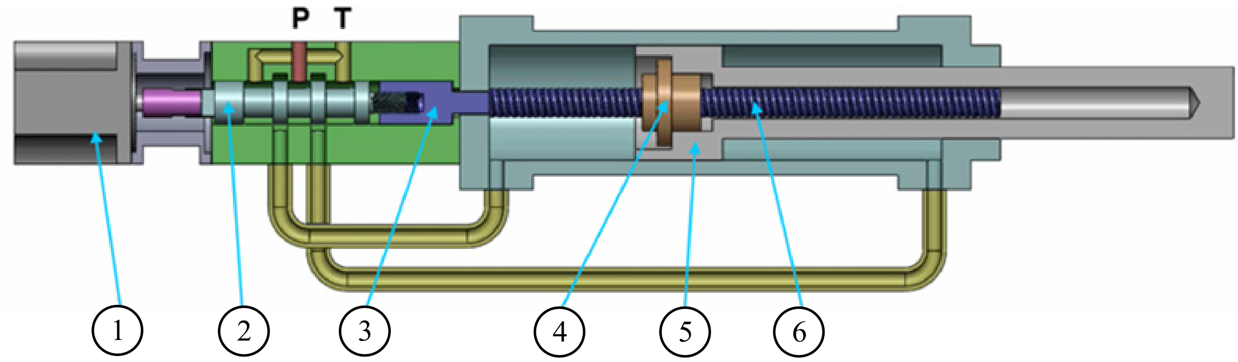

Figure 2. Structure diagram of a digital hydraulic cylinder. 1. Electrically controlled stepping motor/servo motor; 2. Valve spool; 3. Nut bushing; 4. Nut; 5. Rod; 6. Screw stem.

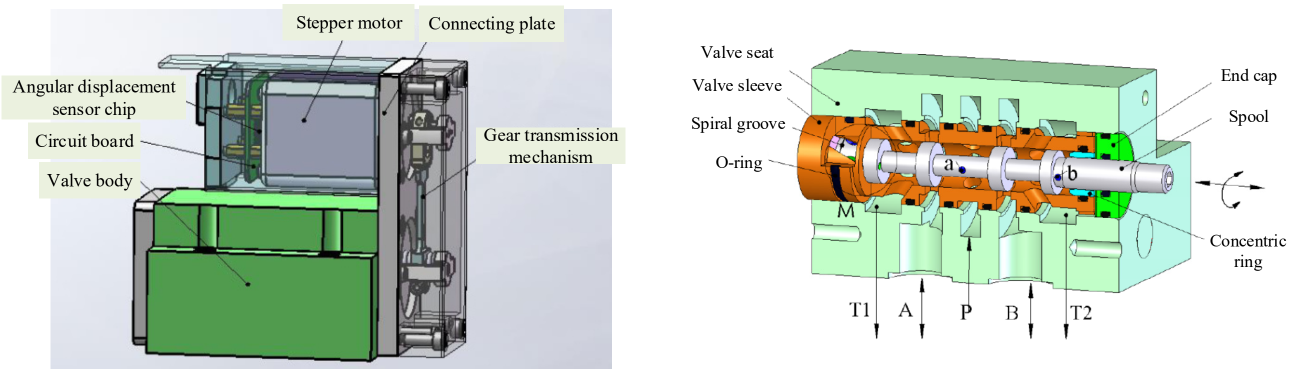

(**a**) (**b**)

Figure 3. Structure diagram of a large-flow digital development valve. (**a**) Structure diagram of digital valve; (**b**) Sectional view of digital valve.

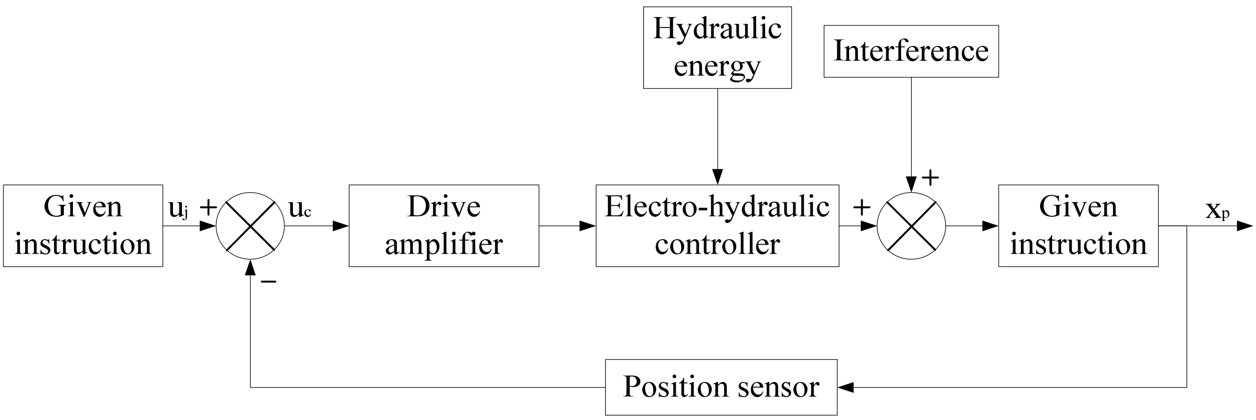

Figure 4. Schematic diagram of a hydraulic cylinder controlled by a traditional servo valve.

2. Working Principle of Hydraulic Cylinder System

The working principle of a hydraulic cylinder is similar to that of an underground mining hydraulic support system, which can be simplified as a valve-controlled cylinder model. The working schematic diagram of the system is shown in Figure 5.

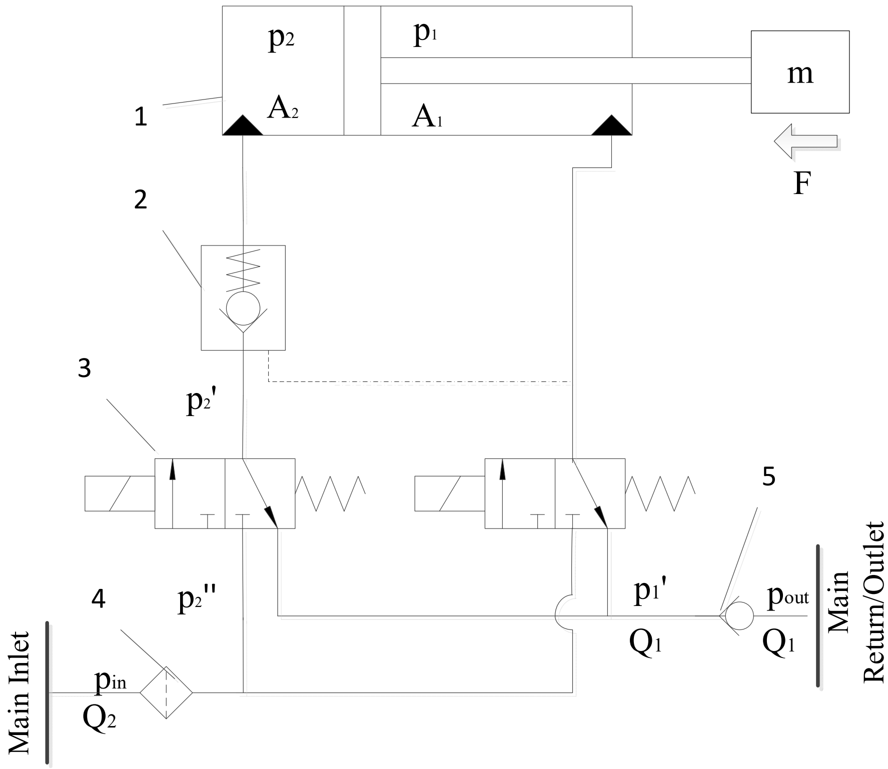

Figure 5. Working principle of a hydraulic cylinder system. 1. Hydraulic cylinder; 2. Liquid control check valve; 3. Directional valve; 4. Filter; 5. Return circuit breaker.

The force balance equation of a hydraulic cylinder when it is under extension and retraction is:

$$p_2 A_2 - p_1 A_1 - F = ma \tag{1}$$

The valve port flow equation is:

$$Q = C_V A \sqrt{\frac{2}{\rho}\Delta p} = k_p \sqrt{\Delta p} \tag{2}$$

Powered on the solenoid valve on the left, the following formula can be derived:

$$Q_2 / Q_1 = A_2 / A_1 \tag{3}$$

$$p_{in} - p_2'' = \Delta p_2'' \tag{4}$$

$$p_2'' - p_2' = \Delta p_2' \tag{5}$$

$$p_2' - p_2 = \Delta p_2 \tag{6}$$

$$Q_2 = k_2'' \sqrt{\Delta p_2''} = k_2' \sqrt{\Delta p_2'} = k_2 \sqrt{\Delta p_2} \tag{7}$$

Combining the above formulas obtains:

$$Q_2 = k_2^x \sqrt{\Delta p_2^x} \tag{8}$$

$$\Delta p_2^x = p_{in} - p_2 \tag{9}$$

$$k_2^x = \sqrt{\frac{1}{\left(\frac{1}{k_2''}\right)^2 + \left(\frac{1}{k_2'}\right)^2 + \left(\frac{1}{k_2}\right)^2}} \tag{10}$$

where Q_2 and Q_1 are the unit inlet and outlet flow, respectively; A_1 is the area of the rod-less chamber of the piston; A_2 is the area of the rod chamber of the piston; p_{in} is the inlet pressure of the system; p_{out} is the outlet pressure of the system; Q is the inlet flow; p_1', p_2' and p_2'' are the pressure behind the return circuit breaker, check valve and filter, respectively; k_2'', k_2' and k_2 are the comprehensive flow coefficient of filter, directional valve and the check valve, respectively; k_2^x is the comprehensive flow coefficient from the inlet to the rod chamber when the hydraulic cylinder extends; $\Delta p_2''$, $\Delta p_2'$ and Δp_2 are the pressure difference of filter, directional valve and check valve, respectively; and Δp_2^x is the pressure drop from the inlet to the rod chamber when the hydraulic cylinder extends.

Similarly, with Equation (7), the outlet flow equation can be deduced as shown below:

$$Q_1 = k_1^x \sqrt{\Delta p_1^x} \tag{11}$$

where Δp_1^x is the pressure drop from the rod-less chamber to the main return when the hydraulic cylinder extends. k_1^x is the comprehensive flow coefficient from the rod-less chamber to the main return when the hydraulic cylinder extends.

$$\Delta p_1^x = p_1 - p_{out} \tag{12}$$

$$k_1^x = \sqrt{\frac{1}{\left(\frac{1}{k_1'}\right)^2 + \left(\frac{1}{k_1}\right)^2}} \tag{13}$$

By solving Equations (1), (3), (8) and (11), the system flow equation can be obtained as follows:

$$Q_2 = \sqrt{(p_{in}A_2 - p_{out}A_1 - F)/[\frac{A_1^3}{(k_1^x)^2(A_2^2)} + \frac{A_2}{(k_2^x)^2}]} = k_s \cdot f_s(p_{in},\ p_{out}) \tag{14}$$

where

$$f_s(p_{in},\ p_{out}) = \sqrt{(p_{in}A_2 - p_{out}A_1 - F)} \tag{15}$$

$$k_s = \sqrt{1/[\frac{A_1^3}{(k_1^x)^2(A_2^2)} + \frac{A_2}{(k_2^x)^2}]} \tag{16}$$

The hydraulic cylinder displacement is the following equation:

$$L = \int_{t_1}^{t_2} \frac{Q_2}{A_2}\, dt \tag{17}$$

Based on the above hydraulic cylinder extension analysis, for a hydraulic cylinder system unit, the directional valve, hydraulic control check valve and pipeline can be regarded as fixed damping structures when the hydraulic cylinder is under extension or retraction. The system inlet flow can be calculated by the inlet and outlet pressure p_{in} and p_{out} of the system. Accordingly, the position of the hydraulic cylinder can be predicted by flow integration.

2.1. Analysis of the Electro-Hydraulic Control Directional Valve Model

The key of the above theoretical analysis is to equate all hydraulic components to a fixed-orifice model. At present, the electro-hydraulic control directional valve structure in the mining hydraulic system is the most superior. The mechanism is analyzed below, and its schematic diagram is shown in the Figure 6.

Working principle: The electro-hydraulic control directional valve is mainly composed of a pilot valve and a main valve. Under initial conditions, the conical surface in the middle of the inlet valve spool 3 is sealed with the right conical of the valve seat 4. When the solenoid valve acts, the inlet at the pilot side enters the control chamber of the directional valve. The pressure in the control chamber first drives the inlet valve spool to the right, which is sealed with the left conical surface of the valve seat and isolates the working chamber from the return chamber. Then, the pressure drives the return valve spool to move to the right. At this time, the inlet chamber is connected with the working chamber to supply the liquid to the working port. When the solenoid valve is powered off, the pressure in the control chamber gradually drops to zero. Due to the hydraulic pressure of the working port and the spring return force acting on the return valve spool, the inlet valve spool and return valve spool are reset.

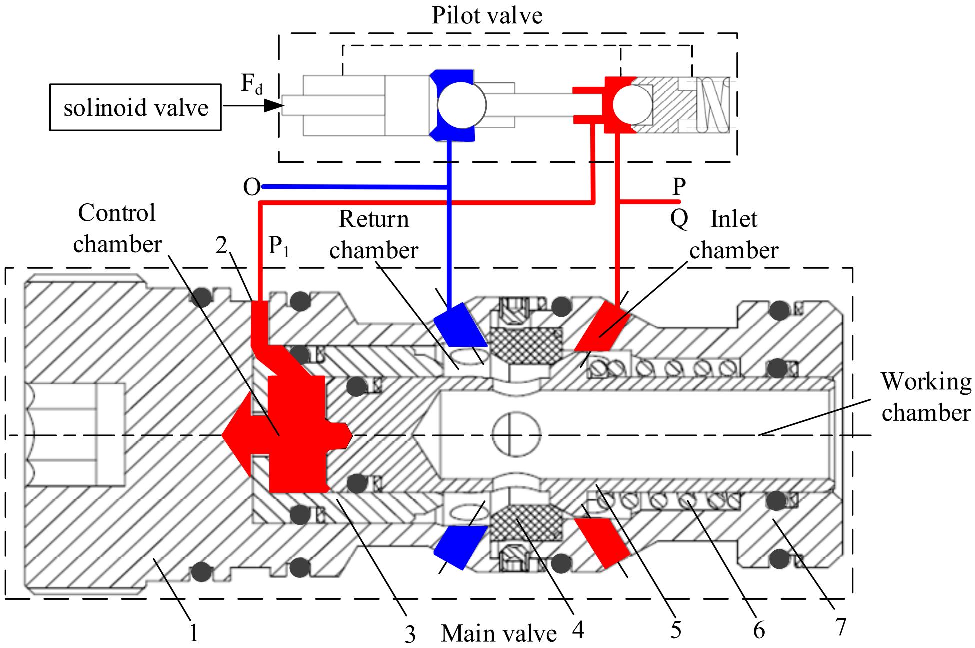

Figure 6. Principle working diagram of a directional valve for hydraulic support. 1. Inlet valve sleeve; 2. Spring; 3. Inlet valve spool; 4. Valve seat; 5. Return valve spool; 6. Fixed orifice; 7. Return valve sleeve.

The ordinary directional valve (also called the ordinary valve) was modeled and analyzed separately, and its equivalent model is shown in Figure 7.

$$p_{tra}(A_D - A_{wrk}) + p_{ctl}A_{ctl} = p_{in}(A_D - A_{wrk}) + p_{wrk}A_{ctl} + F_{sw} + F_{spring} + m(\frac{dx}{dt})^2 \quad (18)$$

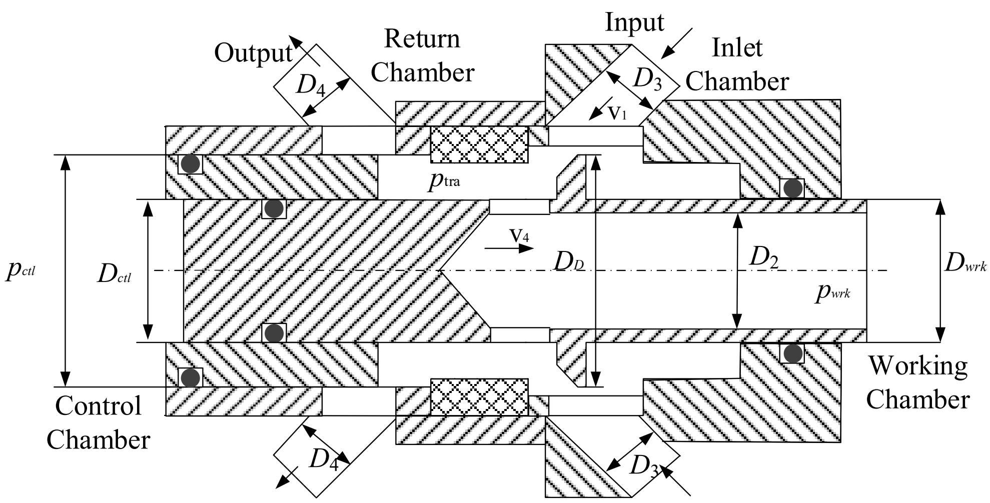

Figure 7. Structural diagram of the ordinary directional valve.

Generally, the opening of the valve spool is relatively small and limited. As long as the hydraulic pressure of the control chamber is greater than those of the inlet chamber, working chamber, hydraulic force and spring return force, the opening can remain unchanged, which can meet the steady-state conditions.

$$p_{tra}(A_D - A_{wrk}) + p_{ctl}A_{ctl} = p_{in}(A_D - A_{wrk}) + p_{wrk}A_{ctl} + F_{sw} + F_{spring} \tag{19}$$

According to the continuity equation of the valve port flow, the following equation is:

$$Q = C_V A_{11}\sqrt{\frac{2(p_{in} - p_{tra})}{\rho}} = C_v A_{22}\sqrt{\frac{2(p_{ctl} - p_{wrk})}{\rho}} \tag{20}$$

Hydrodynamic force mainly considers steady-state hydrodynamic force, which is mainly related to the change in direction. It is obtained according to the momentum theorem.

$$F_{SW} = \rho Q_v v_4 + \rho Q_v v_1 \cos\beta = 2(c_v A_{22})^2(p_{tra} - p_{wrk})(\frac{1}{A_d} + \frac{\cos\beta}{A_{11}}) \tag{21}$$

Under steady-state conditions, the control chamber pressure is equal to the inlet chamber pressure, and it can be seen that:

$$C_1 A_{11}^3 - \cos\beta \cdot A_{11}^2 + (A_{22}^2 - f(p_{wrk}))A_{11} = \cos\beta \cdot A_2^2 \tag{22}$$

where

$$C_1 = \frac{A_{ctl}}{2(c_v A_{22})^2} - \frac{1}{A_d} \tag{23}$$

$$f(p_{wrk}) = \frac{A_{22}^2(p_{in} - p_{wrk})(A_D - A_{wrk}) + F_{spring}}{2(c_v A_{22})^2(p_{ctl} - p_{wrk})} \tag{24}$$

The meaning of all symbols is shown in Table 1.

Table 1. Formula variable table.

Symbol	Name	Unit	Remark
A_{11}	Sealing cross-sectional area	mm^2	
A_{22}	Area of inlet valve spool liquid through holes	mm^2	
F_{spring}	Spring pre-compression force	N	
A_D	Outer hole area of inlet valve spool	mm^2	
A_d	Inner hole area of inlet valve spool	mm^2	
p_{in}	Inlet pressure	MPa	
p_{wrk}	Working port load pressure	MPa	
p_{ctl}	Control port pressure	MPa	
p_{tra}	Transition pressure	MPa	
β	Coaxial angle of liquid inlet direction	$^\circ$	Degree
c_v	Valve port flow coefficient	1	
Q	Inlet flow	L/min	
x	Valve spool displacement	mm	

In the general hydraulic control system, the working face is controlled by constant pressure, i.e., p_{in} is constant and set to 30 MPa. In order to verify the relationship between the valve spool opening and the inlet working pressure, when the working pressure gradually increases from zero to system pressure 30 MPa, the structural parameters of the electro-hydraulic control directional valve are substituted into it. The univariate cubic equation was solved by MATLAB, only the real solution was retained for analysis and the data was analyzed and sorted. The data diagram is shown in Figure 8.

As can be seen, Figure 8 is divided into three zones according to valve spool structural characteristics. The first zone is normally open. In the initial stage, the working port pressure is zero, and the hydrodynamic force is zero. At this time, the hydraulic driving force of the control port is significantly greater than the hydraulic force of the valve spool closing, which causes the spool to open. When the system pressure is lower than 10 MPa, the driving force of the control chamber is significantly greater than the closing force of the working chamber. At this time, the valve spool opening is equal to 10 mm, which is a fully open area. As the working pressure of the system continues to increase, the opening of the valve spool gradually decreases to reduce the hydraulic force and reset force. This area is a variable opening area. The opening varies according to the working pressure of the system. When the working pressure increases to 29 MPa, the force of the control chamber is less than the combined force of the working chamber force, spring return force and hydraulic force, and the valve spool is nearly closed. When the working pressure of the system exceeds 29 MPa, the stroke is negative. Due to the limit function of the valve seat, it is a closed area. Thus, the opening of the directional valve is dependent on different loads and nonlinear factors such as friction and hydrodynamic force. The reason is that the action area of the control chamber is the same as that of the working port.

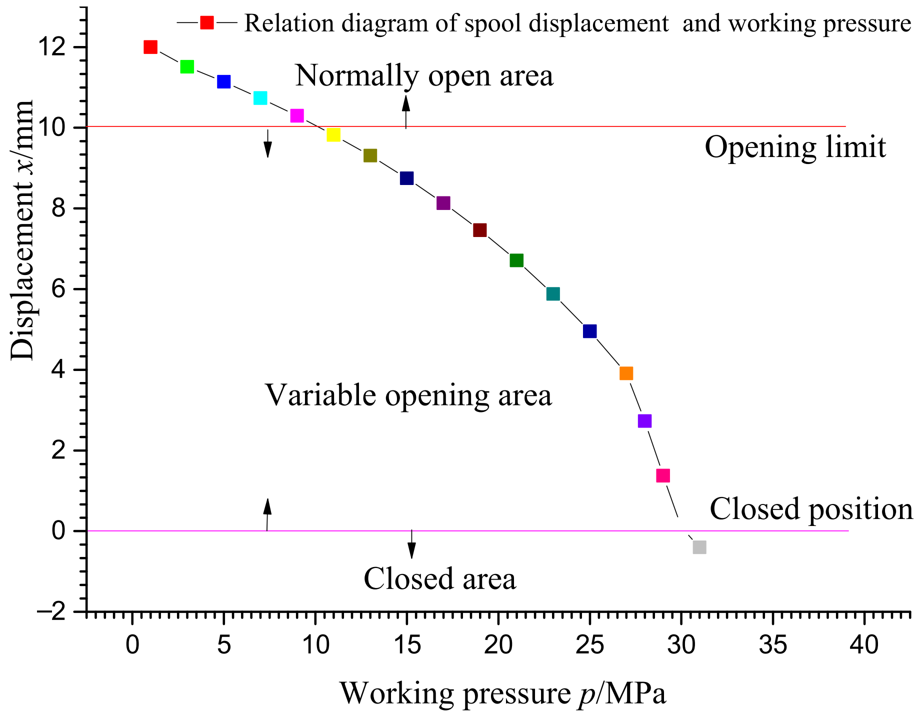

Figure 8. Relationship between working pressure and valve spool opening of the ordinary valve.

In order to solve the above problems, the differential directional valve (also called the differential valve) was proposed to replace the ordinary valve. The main differences of the differential valve are shown in Figure 9. The return valve spool and the inlet valve spool move at the same time when they are in open position, and their equivalent driving area is much larger than the hydraulic action area of the working port. Thus, it can effectively ensure that the hydraulic driving force is much larger than the force in the closing direction and ensure that the opening of the valve spool remains unchanged.

$$p_{tra}(A_D - A_{wrk}) + p_{ctl}A_{ctl} > p_{in}(A_D - A_{wrk}) + p_{wrk}A_{ctl} + F_{sw} + F_{spring} \quad (25)$$

By substituting the structural parameters of the directional valve spool for solution, the relationship between its working pressure and the opening of the valve spool can be obtained. It can be seen from the Figure 10 that, under the full pressure range, the theoretical opening of the system is much larger than the opening limit of the valve. Therefore, the valve is in fully open mode under the working pressure, which is equivalent to the fixed throttle port for modeling and calculation in the commutation process.

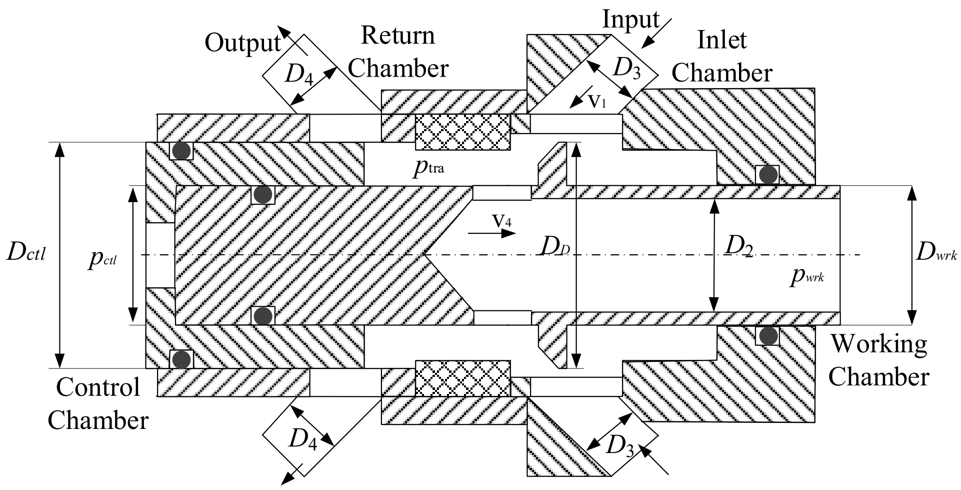

Figure 9. Schematic diagram of the differential directional valve.

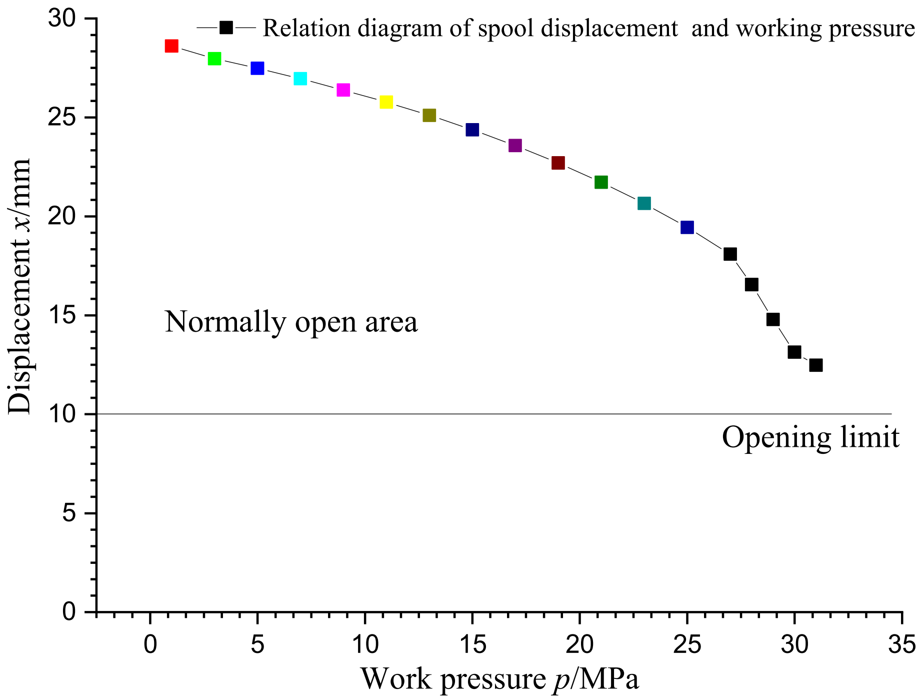

Figure 10. Relationship between working pressure and valve opening of the differential valve.

2.2. Test System of Valve-Controlled Cylinder

In order to analyze and verify the deduced model, a hydraulic cylinder test system was built. The schematic diagram of the experiment is shown in Figure 11. The liquid inlet of the directional valve was connected to the emulsion pump. The working port A1 of the directional valve was connected to the upper chamber of the hydraulic cylinder. The working port A2 of the directional valve was connected to the positive inlet of the hydraulic check valve. The control channel of the hydraulic check valve was connected to the hydraulic cylinder rod chamber. Pressure sensors were connected to the directional valve inlet, directional valve working ports A1 and A2, the upper chamber of the cylinder and the lower chamber of the cylinder to detect pressure changes under different test conditions. A flowmeter was set in the main return liquid to detect the system flow. A laser displacement sensor was installed 1000 mm in front of the hydraulic cylinder for displacement measuring. The acquisition frequency of the test system was 2 kHz. The test equipment parameters are shown in Table 2. The experimental pipeline connection is shown in Figure 12.

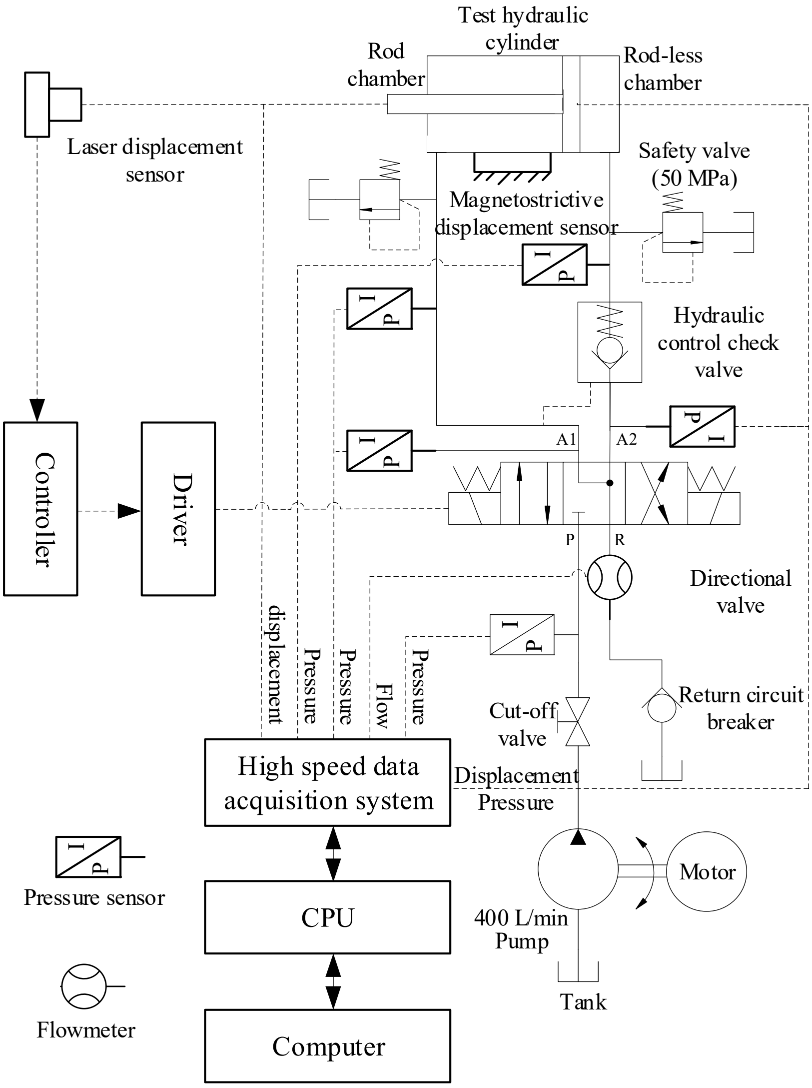

Figure 11. Hydraulic schematic diagram of the test system.

Table 2. Equipment parameters.

Equipment	Parameter	Model
Pump	Nominal flow 200 L/min, nominal pressure 37.5 MPa	BRW200/37.5
Pressure sensor	Measurement range 0–40 MPa, measurement accuracy 0.25%	HDA4846-A-400-000
Return circuit breaker	Nominal flow 200 L/min, nominal pressure 16 MPa	FD200/16
Directional valve	Nominal flow 200 L/min, nominal pressure 31.5 MPa	FHS200/31.5
Hydraulic control check valve	Nominal flow 200 L/min, nominal pressure 50 MPa	FDYA200/31.5
Laser displacement sensor	Measurement 1600 mm, precision ±1 mm	DAN-10-150
Hydraulic cylinder	Cylinder/rod diameter 180/120 mm, stroke 900 mm	TMQTC(180/120*900)

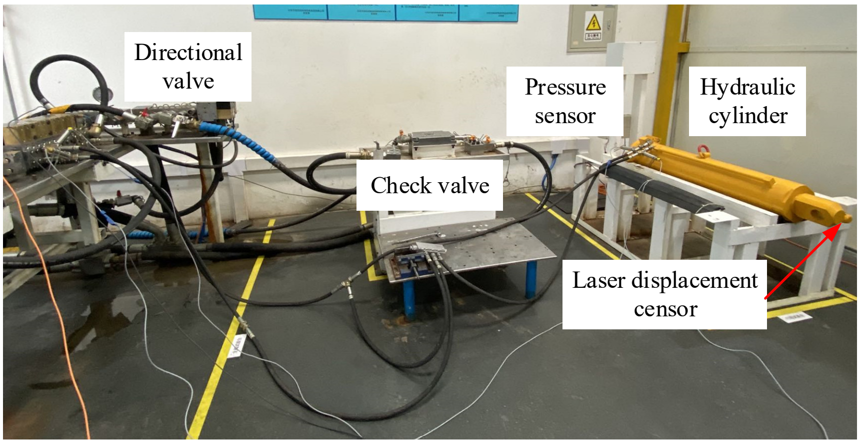

Figure 12. Connection of the hydraulic cylinder system.

3. Results and Discussion

3.1. Verification of the Directional Valve Model

In order to verify the flow resistance characteristics of ordinary valve and differential valve, we collected inlet and outlet pressure and flow data at 5, 10, 15, 20, 25 and 30 MPa from the system under the extension and retraction states of hydraulic cylinder. The experimental results are shown in Tables 3 and 4 below.

Table 3. Hydraulic cylinder retraction data between ordinary valve and differential valve.

System Pressure (MPa)	System Flow (L/min)	Square Root of Pressure Drop (MPa)	
		Ordinary Valve	Differential Valve
6	21.57	1.37	0.37
10.5	41.50	1.36	0.51
17	64.20	0.88	0.64
21.4	72.99	1.11	0.68
26.8	83.81	1.16	0.73
31	92.48	0.79	0.77

Table 4. Hydraulic cylinder extension data between ordinary valve and differential valve.

System Pressure (MPa)	System Flow (L/min)	Square Root of Pressure Drop (MPa)	
		Ordinary Valve	Differential Valve
6	20.62	1.31	0.36
10.5	35.08	1.32	0.47
17	49.94	1.23	0.56
21.4	56.65	1.40	0.60
26.8	64.84	1.61	0.64
31	70.23	1.75	0.67

Figure 13 shows the relationship between the flow and the square root of the pressure drop of the ordinary valve and the differential valve when the hydraulic cylinder was tested under a DN10 diameter pipeline. When the hydraulic cylinder retracted and extended, for the ordinary valve, the linearity of the system flow and the square root of the inlet and outlet pressure drop had obvious randomness. The main reason is that the opening of the ordinary valve was different under different flow conditions. For the differential valve, the linearity of the system flow with the square root of the inlet and outlet pressure drop was high. The main reason is that the differential valve was in a fully open state, which can be modeled as a fixed damping hole. In order to perform the follow-up experiments, the differential valve was taken as the experimental object in the follow-up test and verification.

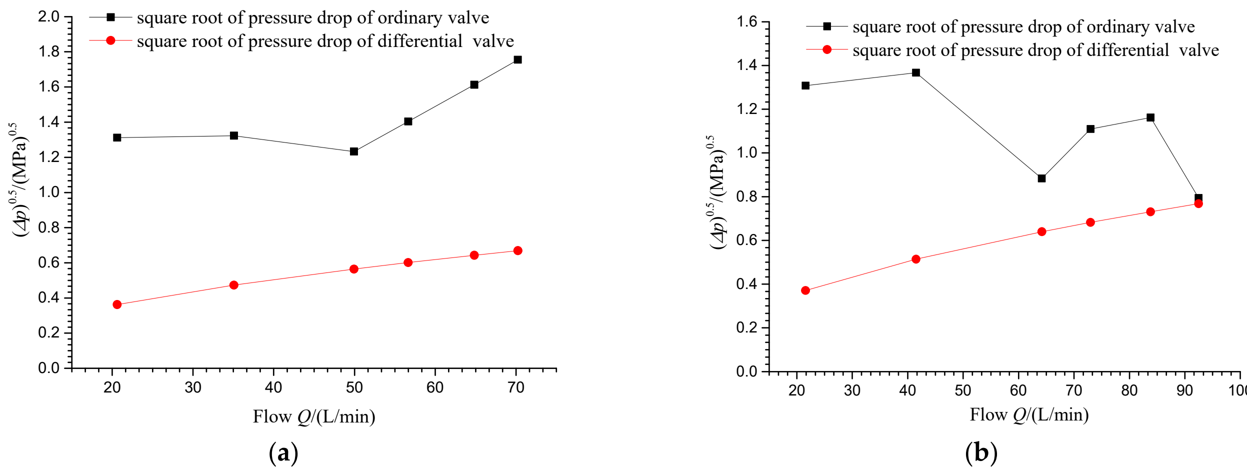

Figure 13. The relationship between flow and square root of pressure drop of ordinary valve and differential valve when hydraulic cylinder is operated; (**a**) Retracted; (**b**) Extended.

3.2. Analysis of System Flow and Inlet and Outlet Pressure of the Experiment Data

The data from under the DN10 pipeline were collected to verify the relationship of system flow, pressure and displacement. The system flow was taken as the *x*-axis, and the inlet and outlet function f(p_{in}, p_{out}) as the *y*-axis when the hydraulic cylinder extended and retracted. The test result is shown in Figure 14.

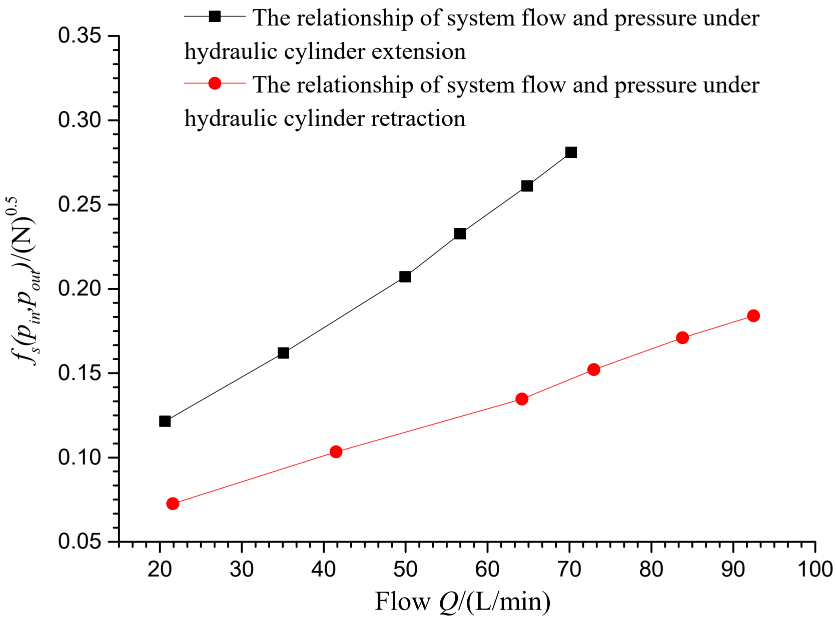

Figure 14. System flow and pressure relationship under DN10 pipeline.

By analyzing Figure 14, it can be seen that the function of inlet/outlet pressure and system flow behaved linearly with a DN10 diameter pipeline. The linearity error was mainly due to friction between the piston and cylinder bore, the change of elastic modulus under different pressure areas and nonlinear operation loads [27]; however, the nonlinearity factors only affected a small portion of the system calibration, so can be ignored.

3.3. Data Verification

According to the measured values of the inlet and outlet pressure sensors, we assigned a value to Equation (15) and calculated the fitting flow of the DN10 diameter pipeline layout under different working conditions. Then, the fitting flow and actual flow were statistically analyzed. Finally, the relative error was calculated. The actual and fitting results are shown in Table 5. The actual and fitting results between flow and pressure are shown in Figure 15.

Table 5. Comparison between fitting flow and actual flow under DN10 pipeline.

	System Pressure (MPa)	5	10	15	20	25	30
Hydraulic cylinder extends under DN10 pipeline	Actual flow (L/min)	20.62	35.08	49.94	56.65	64.84	70.23
	Fitting flow (L/min)	23.16	39.04	49.89	56.15	62.90	67.72
	Relative error (%)	12.32	11.29	0.11	0.88	2.99	3.57
Hydraulic cylinder retracts under DN10 pipeline	Actual flow (L/min)	21.57	41.5	64.2	72.99	83.81	92.48
	Fitting flow (L/min)	25.894	47.234	64.53	72.656	81.738	87.952
	Relative error (%)	20.05	13.82	0.51	0.46	2.47	4.90

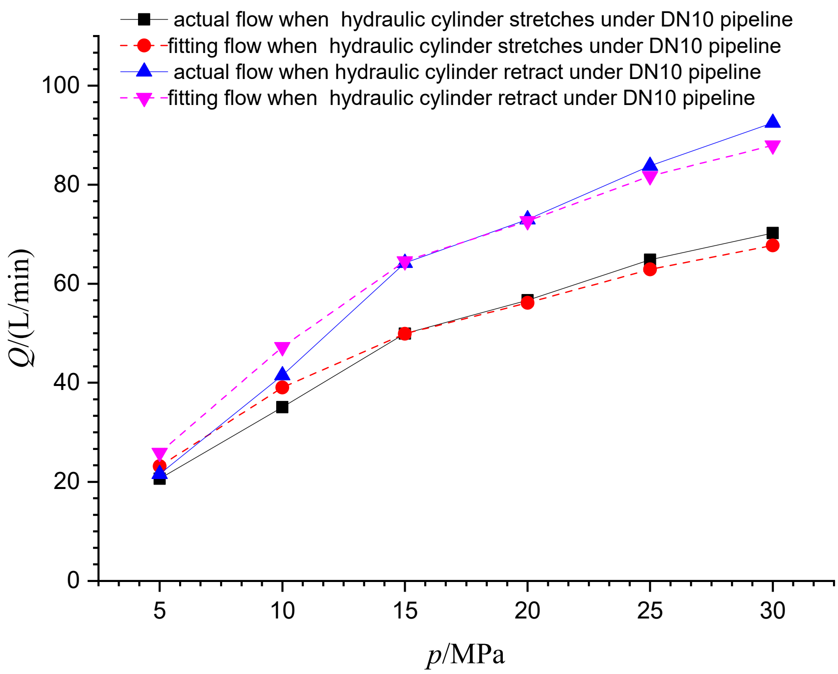

Figure 15. Comparison diagram of fitting flow and actual flow under DN10 diameter pipeline when the hydraulic cylinder extended and retracted.

As is shown in Table 5 and Figure 15, the correlation degree of the fitting flow and actual flow under the DN10 pipeline was good. When the system pressure was over 10 MPa, the relative error of the system flow was within 5%. However, the relative error of system flow reached up to 20% when the system pressure was less than 10 MPa. The reason is mainly due to the change of the elastic modulus under low system pressure. When the system pressure was over 10 MPa, the elastic modulus was approximate to a certain constant. In the next step, we will conduct a quantitative study on nonlinear factors, such as the elastic modulus of the low-pressure zone, to ensure fitting accuracy within the full pressure difference range.

4. Conclusions

A theoretical model of flow and displacement control based on inlet and outlet pressure detection was deduced, and the feasibility in the application scenario without displacement sensor was preliminarily verified. In order to prove the relationship between system flow and inlet and outlet pressure, a test platform was built, and a comparative verification was carried out. The result shows that, compared with an ordinary directional valve, a differential valve has better linearity with regard to pressure and flow characteristics and can be analyzed as fixed damping. When the system pressure is larger than 10 MPa, the system flow can be well fitted with the inlet and outlet pressure drop within 5% of the actual error. This experiment verifies the feasibility of position control through pressure detection of the control hydraulic system by implementing an on–off valve. The verification of this principle provides a new solution for the precise control of the hydraulic support on a fully mechanized working face.

Author Contributions: Conceptualization, R.Z. and X.Y.; methodology, R.Z.; validation, L.M.; formal analysis, R.Z.; investigation, L.M.; resources, R.Z. and X.Y.; data curation, R.Z. and L.M.; writing—original draft preparation, R.Z.; writing—review and editing, L.M.; supervision, R.Z.; project administration, R.Z. and X.Y.; funding acquisition, R.Z. All authors have read and agreed to the published version of the manuscript.

Funding: This research was funded by Beijing Tianma Intelligent Control Technology Co., Ltd., grant numbers 2022TM010-J1 and 2022TM015-J1.

Institutional Review Board Statement: Not applicable.

Informed Consent Statement: Not applicable.

Data Availability Statement: Not applicable.

Acknowledgments: We acknowledge the funding support from Beijing Tianma Intelligent Control Technology Co., Ltd. (project account codes: 2022TM010-J1 and 2022TM015-J1) for this research.

Conflicts of Interest: The authors declare no conflict of interest.

References

1. Wang, G.; Liu, F.; Pang, Y.; Ren, H.; Ma, Y. Coal mine intellectualization: The core technology of high quality development. *J. China Coal Soc.* **2019**, *44*, 349–357. [CrossRef]
2. Wang, G.; Du, Y.; Ren, H.; Fan, J.; Wu, Q. Top level design and practice of smart coal mines. *J. China Coal Soc.* **2020**, *45*, 1909–1924.
3. Marina, R.; Dmitriy, R.; Dmitriy, K.; Tyulenev, M.; Zhironkin, S.; Khoreshok, A. Intelligent mining engineering systems in the structure of industry 4.0. *E3s Web Conf.* **2017**, *21*, 01032.
4. Li, J.; Zhan, K. Intelligent mining technology for an underground metal mine based on unmanned equipment. *Engineering* **2018**, *4*, 381–391. [CrossRef]
5. Yan, S.; Xu, G.; Fan, Z. Development course and prospect of the 50 years'comprehensive mechanized coal mining in China. *Coal Sci. Technol.* **2021**, *49*, 1–9.
6. Song, Z. Application of LASC technology in mine's automatic mining of fully mechanized mining face. *Shenhua Sci. Technol.* **2018**, *16*, 26–29.
7. Li, S. Measurement & control and localisation for fully-mechanized working face alignment based on inertial naviga tion. *Coal Sci. Technol.* **2019**, *47*, 169–174.
8. Zhong, Q.; Zhang, B.; Yang, H.Y.; Ma, J.E.; Fung, R.F. Performance analysis of a high-speed on/off valve based on an intelligent pulse-width modulation control. *Adv. Mech. Eng.* **2017**, *9*, 1–11. [CrossRef]
9. Bruno, N.; Zhu, Y.; Liu, C.; Gao, Q.; Li, Y. Development of a piezoelectric high speed on/off valve and its application to pneumatic closed-loop position control system. *J. Mech. Sci. Technol.* **2019**, *33*, 2747–2759. [CrossRef]
10. Gao, Q. Nonlinear Adaptive Control with Asymmetric Pressure Difference Compensation of a Hydraulic Pressure Servo System Using Two High Speed On/Off Valves. *Machines* **2022**, *10*, 66. [CrossRef]
11. Zhou, G.R.; Liu, S.Q.; Sang, Y.J.; Wang, X.D.; Jia, X.P.; Niu, E.Z. LPV robust servo control of aircraft active side-sticks. *Aircr. Eng. Aerosp. Technol.* **2020**, *92*, 599–609. [CrossRef]
12. Tang, S.; Zhu, Y.; Yuan, S. Intelligent Fault Identification of Hydraulic Pump Using Deep Adaptive Normalized CNN and Synchrosqueezed Wavelet Transform. *Reliab. Eng. Syst. Saf.* **2022**, *224*, 108560. [CrossRef]
13. Deng, Z.Y.; Liu, X.R.; Zhou, X.H.; Yang, Q.H.; Chen, P.; de la Fuente, A.; Ren, L.X.; Du, L.B.; Han, Y.F.; Xiong, F.; et al. Main engineering problems and countermeasures in ultra-long-distance rock pipe jacking project: Water pipeline case study in Chongqing. *Tunn. Undergr. Space Technol.* **2022**, *123*, 104420. [CrossRef]
14. Luo, S.Q.; Cheng, M.; Ding, R.Q.; Wang, F.; Xu, B.; Chen, B.K. Human-Robot Shared Control Based on Locally Weighted Intent Prediction for a Teleoperated Hydraulic Manipulator System. In *IEEE-Asme Transactions on Mechatronics*; IEEE: New York, NY, USA, 2022.
15. Cheng, M.; Han, Z.N.; Ding, R.Q.; Zhang, J.H.; Xu, B. Development of a redundant anthropomorphic hydraulically actuated manipulator with a roll-pitch-yaw spherical wrist. *Front. Mech. Eng.* **2021**, *16*, 698–710. [CrossRef]
16. Gao, Q.; Zhu, Y.; Liu, J.H. Dynamics Modelling and Control of a Novel Fuel Metering Valve Actuated by Two Binary-Coded Digital Valve Arrays. *Machines* **2022**, *10*, 55. [CrossRef]

17. Zhong, Q.; Wang, X.; Zhou, H.; Xie, G.; Hong, H.; Li, Y.; Chen, B.; Yang, H. Investigation Into the Adjustable Dynamic Characteristic of the High-Speed on/off Valve With an Advanced Pulsewidth Modulation Control Algorithm. In *IEEE/ASME Transactions on Mechatronics*; IEEE: New York, NY, USA, 2021; pp. 1–14.
18. Zhou, R.; Li, S.; Wei, W.; Zhang, L.; Wang, W. Study on coupling mechanism of pressure and flow in following hydraulic system of mining face. *Coal Sci. Technol.* **2020**, *48*, 129–136.
19. Zhou, R.; Meng, L.; Yuan, X.; Qiao, Z. Research and experimental analysis of hydraulic cylinder position control mechanism based on pressure detection. *Machines* **2021**, *10*, 1. [CrossRef]
20. Yang, H.; Guo, Y.; Zhang, H.; Wang, X.; Lin, B.; Dang, Y. Development of the hydraulic cylinder position control system based on electromagnetic directional valve. *Mach. Des. Manuf. Eng.* **2020**, *49*, 101–104.
21. Venkata, S.K.; Rao, S. Fault Detection of a Flow Control Valve Using Vibration Analysis and Support Vector Machine. *Electronics* **2019**, *8*, 1062. [CrossRef]
22. Jia, W.; Ruan, J. A new kind of digital on-off valve with high flow rate. *J. Zhejiang Univ. Technol.* **2017**, *45*, 137–141.
23. Zhou, C.; Wen, G.; Qing, X. Study of electro-hydraulic position control system using solenoid directional valve. *Eng. J. Wuhan Univ.* **2017**, *50*, 760–765.
24. Jin, L. *Study on the Precise Position Control of Hydraulic Cylinder Using Solenoid Operated Directional Control valve*; Zhejiang University: Hangzhou, China, 2019.
25. Pan, M.; Plummer, A.; El Agha, A. Theoretical and Experimental Studies of a Switched Inertance Hydraulic System in a Four-Port High-Speed Switching Valve Configuration. *Energies* **2017**, *10*, 780. [CrossRef]
26. Masood, K.; Dauptain, X.; Zoppi, M.; Molfino, R. Hydraulic Pressure-Flow Rate Control of a Pallet Handling Robot for an Autonomous Freight Delivery Vehicle. *Electronics* **2020**, *9*, 1370. [CrossRef]
27. Yuan, X.; Wang, W.; Zhu, X. Theory Model of Dynamic Bulk Modulus of Aerated Hydraulic Fluid. *Chin. J. Mech. Eng.* **2022**. [CrossRef]